



Published in final edited form as:

Anal Chem. 2011 February 15; 83(4): 1180–1184. doi:10.1021/ac103070t.

Increased *In Vivo* Glucose Recovery via Nitric Oxide Release

Scott P. Nichols^{*}, Nga N. Le[†], Bruce Klitzman[†], and Mark H. Schoenfisch^{*}

^{*}Department of Chemistry, University of North Carolina at Chapel Hill, Chapel Hill, NC 27599

[†]Kenan Plastic Surgery Research Labs and Department of Biomedical Engineering, Duke University Medical Center, Durham, NC 27710

Abstract

The *in vivo* glucose recovery of subcutaneously implanted nitric oxide (NO)-releasing microdialysis probes was evaluated in a rat model using saturated NO solutions to steadily release NO. Such methodology resulted in a constant NO flux of 162 pmol cm⁻² s⁻¹ from the probe membrane over 8 h of perfusion daily. The *in vivo* effects of enhanced localized NO were evaluated by monitoring glucose recovery over a 14 d period, with histological analysis thereafter. A difference in glucose recovery was observed starting at 7 d for probes releasing NO relative to controls. Histological analysis at 14 d revealed lessened inflammatory cell density at the probe surface and decreased capsule thickness. Collectively, the results suggest that intermittent sustained NO release from implant surfaces may improve glucose diffusion for subcutaneously-implanted sensors by mitigating the foreign body reaction.

INTRODUCTION

The development of implantable glucose sensors that function for extended durations (>1 week) remains elusive primarily due to the foreign body reaction (FBR).^{1, 2} It is now well known that the FBR is initiated upon protein adsorption to the implant and culminates with the formation of a fibrous capsule that sequesters the implant from normal tissue.^{3–6} The acute inflammatory response also has a significant effect on the long-term FBR and sensor function.⁷ The unfortunate isolation of implanted sensors via the FBR results in decreased analyte diffusion and analytical performance.^{3, 8, 9} Achieving extended sensor lifetimes requires strategies for mitigating the FBR and improving tissue integration. Prior examples of such strategies include the use of more hydrophilic interfaces, porous coatings, and surfaces that release pro-angiogenic factors and collagen inhibitory agents.^{10–12} Although some improvements in mitigating the FBR have been reported, none have fully resolved the problems that reduce the sensor lifetime *in vivo*.

Nitric oxide (NO) is an endogenously produced molecule that acts as a signaling molecule for cytokine production and has been used to reduce bacterial and platelet adhesion.^{13–17} *In vivo*, active release of NO from a surface has been shown to reduce bacterial adhesion/infection and improve implant-tissue integration by reducing inflammatory cell infiltration and collagen encapsulation.^{18–21} In these studies, release of NO in the first days of implantation significantly changed both the short- and long-term inflammatory response.^{18, 21} As such, NO release has the potential to address the difficulties with the FBR associated with subcutaneous sensor platforms and improve sensor function.

The positive effects of NO release on the FBR have not been assessed with respect to analyte diffusion through the developing capsule. Our hypothesis is that a thinner capsule may result in enhanced glucose diffusion thus improving one facet of sensor performance. Microdialysis allows for direct quantification of glucose diffusion through a membrane during the FBR. Probes are calibrated by evaluating the extraction efficiency (EE, eq 1) of a

given analyte.^{22, 23} The EE is calculated using the concentration of analyte in the perfusate, dialysate and external solution represented by C_p , C_d and C_e , respectively. The resistances to mass

$$EE = \frac{C_d - C_p}{C_e - C_p} = 1 - \exp\left(\frac{-1}{Q_d (R_m + R_d + R_{bf} + R_{eo} + R_{tr})}\right) \quad (1)$$

transfer through the membrane (R_m) and dialysate (R_d) are intrinsic to the individual probe and can be accounted for by *in vitro* calibration.²² The external resistances to mass transfer of biofouling (R_{bf}), encapsulation (R_{ec}) and tissue trauma layers (R_{tr}) are dependent on the host response to the probe once implanted, and may change with time.²³⁻²⁶ Glucose consumption may also be increased in wounded tissue and is thus included in the tissue trauma term.²⁷

As with subcutaneous sensors, microdialysis probes suffer from diminished analyte diffusion with longer implantation time.^{11, 26, 28} Stenken et al. previously examined the effect of the FBR on analyte diffusion through a microdialysis membrane using magnetic resonance.²⁹ Others have evaluated membrane composition and the active release of vascular endothelial growth factor (VEGF) or dexamethasone to alter analyte recovery.^{11, 26, 29} Neither altering membrane composition nor VEGF or dexamethasone release were found to adequately circumvent the effect that the FBR has on analyte diffusion. Herein, we evaluate the influence of NO release on glucose recovery using microdialysis probes implanted subcutaneously in a rodent model.

EXPERIMENTAL SECTION

Reagents and Materials

Nitrogen, argon and nitric oxide were purchased from AirGas National Welders (Raleigh, NC). Glucose, glucose oxidase (type VII-S from *Aspergillus niger*; 168800 units/g) and horseradish peroxidase (type I, 118 units/mg) were purchased from Sigma (St. Louis, MO). CMA/20 microdialysis probes with a 10 mm polyarylethersulfone (PAES) membrane and 20-kDa molecular weight cutoff were purchased from CMA Microdialysis Inc (North Chelmsford, MA). Bioanalytical Systems (West Lafayette, IN) Baby Bee syringe pumps with 3-syringe brackets, 1 mL Bee Stinger syringes, FEP tubing, PEEK tubing and microdialysis connectors were used to perfuse microdialysis probes. O-dianisidine dihydrochloride was obtained from Alfa Aesar (Ward Hill, MA). All other reagents used were reagent grade and used as received. Phosphate buffered saline (PBS; 10 mM, pH 7.4) was prepared in-house. PBS saturated with NO (PBS-NO; 1.9 mM NO) was prepared by purging approximately 20 mL of PBS with argon gas for 20 min to remove oxygen, followed by nitric oxide gas for 20 min. The solution was stored at 4 °C and used up to 48 h after saturation.

Measurement of NO release

Real-time NO release was collected using a Sievers 280 Chemiluminescent NO Analyzer (Boulder, CO). The instrument was calibrated with an atmospheric sample that had been passed through an NO zero filter and a 25.6 ppm NO gas standard (balance N_2). Nitric oxide release from the microdialysis probe was measured by immersing the probe in deoxygenated PBS at 37 °C. PBS-NO was then perfused through the probe at 2.0 μ L/min with NO carried from the buffer to the NO Analyzer by a stream of N_2 bubbled into the solution at a flow rate of 80 mL/min.

***In Vitro* Glucose Recovery**

Prior to implantation, microdialysis probes were sterilized with ethylene oxide (gas treatment), out-gassed for 7 d to facilitate ethylene oxide desorption, and subsequently hydrated in sterile PBS for 24 h. Probes were then calibrated in a well-stirred solution of sterile 5.5 mM glucose in PBS at a flow rate of 2.0 $\mu\text{L}/\text{min}$ with PBS or PBS-NO as the perfusate. Three separate dialysates were collected from each probe and stored at $-20\text{ }^{\circ}\text{C}$ until analysis.

Implantation and *In Vivo* Perfusion of Probes

The animal protocol used in this study was approved by an IACUC committee at Duke University. Microdialysis probes were implanted into adult male CD rats (150-200 g) purchased from Charles River Laboratories (Raleigh, NC). Rats were anesthetized with 2-4% isoflurane (v/v in O_2). Two probes (one control and one NO-releasing) were then implanted subcutaneously in 10 rats. Probes were placed bilaterally 5-7 cm caudal to the scapulae, approximately 2 cm lateral to the spine, in the dorsal subcutis with the probe tips oriented caudally, and the inflow and outflow percutaneous catheters at the base of the neck.

PEEK or FEP tubing was used with control probes. PEEK tubing was connected to the inlet of the NO-releasing probes because of its low permeability to NO. Rats were fitted into infusion harnesses with a spring offset attached to a dual-channel stainless steel swivel on a counter-balanced swivel mount (Instech Laboratories, Plymouth Meeting, PA) to allow free movement while continuously perfusing probes. Immediately following implantation and for each subsequent day, probes were perfused at 2.0 $\mu\text{L}/\text{min}$ for 8 h with test (NO gas) or blank perfusate. During the last 15 min of the perfusion period, one dialysate sample was collected every 5 min and stored at $-20\text{ }^{\circ}\text{C}$. Immediately following sample collection, a blood sample was taken via the rat tail vein to allow for blood glucose measurement using a OneTouch Ultra glucose test strip with a OneTouch Ultra Glucometer (LifeScan, Milpitas, CA).

Explantation and Fixation of Capsules

After 14 d, or after both probes failed, rats were anesthetized with 2-4% isoflurane (v/v in O_2) to allow explantation of the probes with the surrounding tissue capsule intact. Microdialysis probes were removed from the capsule if still functional and placed in PBS. The capsules were placed in 10% buffered formalin (v/v) for 24 h and then transferred to 70% ethanol for 24 h prior to their embedment into paraffin. Sections of the paraffin embedded capsule were stained with Masson's trichrome or hematoxylin and eosin (H&E) for analysis. Images of the trichrome and H&E stained samples were collected using 4x, 10x and 20x objectives on a Nikon Eclipse TE2000-U with a Nikon Digital Sight DS-2Mv Digital Camera (Nikon Inc., Melville, New York).

Glucose Detection

All glucose samples were measured using a colorimetric glucose assay in a 96-well microtiter plate format. Phosphate buffer (58.5 μL , pH 7.0) was added to each microtiter plate followed by addition of either dialysate (3 μL) or varying volumes of a standard glucose solution (1-3 μL) for a calibration curve. In the dark, a glucose assay mix (58.5 μL , pH 7.0) containing glucose oxidase (17.2 U/mL), horseradish peroxidase (3.6 U/mL) and o-dianisidine (0.43 mM) was added to each well and incubated at $37\text{ }^{\circ}\text{C}$ for 1 h. After incubation, 12 N sulfuric acid (80 μL) was added to end the reaction and intensify the color. The absorbance of each well was measured using a Labsystems Multiskan RC microplate reader (Helsinki, Finland) equipped with a 540 nm filter.

Histology Analysis

Histological analysis was performed on tissue adjacent to probes functional ≥ 13 d of implantation. Capsule thickness was measured from trichrome-stained tissue sample. The foreign body capsule was defined as the region of inflammatory cells at the probe surface and the dense collagen oriented parallel to the probe membrane. Two cross-sectional slides per capsule were imaged with seven measurements of the capsule thickness per image and averaged. Collagen density was calculated in four $400 \times 100 \mu\text{m}^2$ fields from each of two slides per probe using a previously developed MATLAB (The MathWorks, Natick, MA) program that determines the percent collagen.^{10, 30} The inflammatory response as determined by cell density was calculated by counting the nuclei between the dense collagen and probe surface in four $50 \times 100 \mu\text{m}^2$ fields from each of two slides per probe using a MATLAB program.^{30, 31}

RESULTS AND DISCUSSION

We and others have reported on the promising anti-infection efficacy of and wound healing properties promoted by materials that spontaneously release NO.^{18, 19, 21} To date, the long-term benefits of NO on *in vivo* sensor or probe response have not been determined despite reduced capsule formation. Microdialysis studies allow for direct quantification of analyte diffusion to the implant surface as a function of implant time, a critical parameter for developing biocompatible *in vivo* sensors. In contrast to standard tissue histology, daily monitoring is feasible as the tissue is not disrupted for analysis, thus requiring fewer animals for a complete study. To evaluate the effect of NO release during the early stages of the wound healing process, an appropriate method for delivering NO was determined.

An initial approach for achieving controlled NO release from a microdialysis probe focused on perfusing small molecule NO donors. Unfortunately, the NO release kinetics from the small molecule NO donors we employed was too rapid, resulting in irregular NO release and even bubble formation in the syringe. Silica-based nanoparticles were also explored due to their extended NO release, but we observed significantly larger probe failure rates attributed to blocking of the probe and/or tubing by particles. Coating NO-releasing polyurethane directly onto the membrane significantly diminished glucose recovery. We thus determined that using saturated NO solutions provided steady, controlled NO release without compromising the probe prior to implantation.

NO Release from Microdialysis Probes

A NO-saturated PBS solution introduced through the microdialysis probe at $2.0 \mu\text{L}/\text{min}$ provided a constant NO flux during the perfusion period (Figure 1). An 8 h perfusion window allowed time for the probes to be disconnected, reducing mechanical stress on the percutaneous implants (mechanical stress has been shown to affect wound healing *in vivo*)¹⁰. In PBS, we measure an average NO flux of $162 \pm 18 \text{ pmol cm}^{-2} \text{ s}^{-1}$, corresponding to a total release of $4.6 \pm 0.5 \mu\text{mol cm}^{-2}$ per day over 14 d of implantation. By releasing NO from the perfusate, we were able to compare the control and NO-releasing probes directly as the membrane material contacting the surrounding tissue remained identical. While constant noise in the NO flux originating from the syringe pump noise was noted, the observed signal was always $>3\sigma$ greater in magnitude (Figure 1).

The measured NO flux was significantly less than expected from the saturated NO solution (1.9 mM NO). While a portion of the decreased NO flux may be attributed to incomplete diffusion of the NO through the probe membrane, flow rate experiments indicated greater loss through the gas permeable microdialysis probe tubing at reduced flow rates (data not shown). To reduce NO loss, we attempted to replace the inlet tubing with gas-impermeable PEEK tubing. Unfortunately, the stiffness of the PEEK tubing led to a greater rate of probe

failure due to undesirable mechanical stress. Although the polyurethane resulted in lower (~60%) NO flux, its use was necessary for enabling a robust set up, with levels of NO similar to our previous NO-releasing xerogel materials that reduced the capsule formation *in vivo*.

Glucose Recovery: *In Vitro* and *In Vivo*

Either the glucose concentration in the external solution (bench studies) or the blood glucose concentration (*in vivo*) were used with the dialysate concentrations (Figure SI-1) to calculate the EE using eq 1 and multiplied by 100 to obtain EE%. Blood glucose levels were used to estimate the glucose concentration in subcutaneous tissue (C_e).³² The EE% for glucose of probes in well-stirred *in vitro* solutions using PBS and PBS-NO was 70 ± 5 and $71 \pm 5\%$, respectively. The observed difference was not statistically significant and allowed for direct comparison between the control and experimental microdialysis probes *in vivo*. While the *in vivo* microdialysis flow rate employed ($2 \mu\text{L}/\text{min}$) may deplete local glucose more rapidly than an implanted electrochemical sensor,²⁷ the steady-state equilibrium established *in vivo* at such a flow rate was necessary to quantify the wound healing response. As shown in Figure 2, the EE% of NO-releasing probes remained constant over the 2 week implantation while control probes suffered from diminished analyte diffusion after 7 d of perfusion. As much prior work has noted that fibrous encapsulation diminishes diffusion of small analytes to implant surfaces, our results may indicate a reduced capsule thickness and ultimately improve sensor performance.³³ Indeed, others have indicated that the lag in sensor response time originates from greater resistance to mass transfer.³⁴ Equally problematic, lowered analyte diffusion through a highly resistive fibrous capsule may interfere with glucose and oxygen levels at the sensor-tissue interface, thereby negatively affecting sensor performance.³⁵ Based on the EE%, we predict that NO-releasing glucose sensor membranes would facilitate enhanced glucose diffusion over long implantation periods compared to controls, and improve sensor performance. Such studies are currently underway in our laboratory.

Histology Analysis

Wang et al. previously reported the encapsulation of their microdialysis probes in a rat model after ~7 d.²⁵ We thus hypothesize that the EE% difference between NO and control probes is the result of decreased microdialysis probe encapsulation from NO release. Histological analysis of the capsules surrounding NO-releasing and control probes is shown in Figure 3. As expected, the thickness of the fibrous capsule surrounding the Masson's trichrome-stained cross sections of control probes (Table 1) was greater than that measured for the NO-releasing probes. The cross sections stained with H&E (Figure 3) also revealed decreased inflammatory cell densities at the NO-releasing probe membranes relative to controls, indicative of a mitigated FBR. Unexpectedly, the collagen density adjacent to NO-releasing was greater than that adjacent to control probes.

The cause for increased collagen density is presently unknown. While we previously reported a decrease in collagen density for NO-releasing xerogel membranes, others have reported that NO at high concentrations increases collagen deposition in wound healing.^{18, 36-38} Of note, the xerogel system resulted in a burst of NO initially followed by significantly less (~95%) NO release for ~3 d. In contrast the NO release levels used in this study were equivalent to daily NO bursts for 8 h. Although improving glucose recovery and reducing the initial FBR, our data indicates that intermittent NO bursts at large NO flux may negatively impact long-term wound reconstruction. Koschwanez et al. have also reported that percutaneous and subcutaneous implants behave differently, possibly due to mechanical stresses.¹⁰ As well, we observed significant migration of the percutaneously-implanted probes during our study, likely caused by animal movement and resulting stress from the

microdialysis tubing. Such stress would augment the FBR to the implanted material. Future studies should examine the effect of NO as a function of implant type (i.e., subcutaneous or percutaneous). Furthermore, NO is a potent vasodilator,³⁹ and the effect of blood flow changes on glucose recovery using microdialysis probes is controversial.^{40–42} However, we note that the glucose recovery in our model was not affected in the acute phase (< 7d) as a function of NO release (Figure 2), indicating no effects due to NO-induced vasodilation. While microdialysis allowed for daily NO release and subsequent analysis of the FBR, probe failure remained a limitation. For example, total microdialysis probe failure rates were ~30 and 65% over 8 and 14 d, respectively. Using these methods, studies lasting ≥14 d would likely suffer similarly high failure rates, regardless of NO release.

CONCLUSIONS

We demonstrated the benefits of *in vivo* NO release using microdialysis with respect to glucose recovery and the FBR. The observed difference in EE% obtained from glucose recovery data suggested improved tissue integration of the microdialysis probe. Histological analysis indicated that the release of NO reduced both the capsule thickness and inflammatory cell density at the surface. While the kinetics and total release of NO employed are not yet achievable through conventional NO storage/release chemistries (e.g., NO donors), our results support the conclusion that NO release is a viable strategy for mitigating the FBR and improving analyte diffusion to a sensor. Future work may determine the optimal NO release flux and durations, and the concomitant effects of NO on long-term tissue viability. By maintaining glucose diffusion to a subcutaneous implanted sensor, both the sensitivity and response time may be enhanced circumventing previous FBR-mediated limitations. Studies evaluating the effects of NO release on the analytical performance of *in vivo* glucose sensors are currently underway.

Supplementary Material

Refer to Web version on PubMed Central for supplementary material.

Acknowledgments

The authors acknowledge research support from the National Institutes of Health (NIH EB000708). The authors also thank Dr. W. Monty Reichert for use of the Nikon Eclipse TE2000-U microscope.

REFERENCES

1. Frost MC, Meyerhoff ME. *Curr Opin Chem Biol* 2002;6(5):633–641. [PubMed: 12413548]
2. Wilson GS, Gifford R. *Biosensors Bioelectron* 2005;20(12):2388–2403.
3. Gifford R, Kehoe JJ, Barnes SL, Kornilayev BA, Alterman MA, Wilson GS. *Biomaterials* 2006; (27):2587–98. [PubMed: 16364432]
4. Ratner BD. *J Controlled Release* 2002;78(1-3):211–218.
5. Ratner BD, Bryant SJ. *Annu Rev Biomed Eng* 2004;6(1):41–75. [PubMed: 15255762]
6. Coleman DL, King RN, Andrade JD. *J Biomed Mater Res* 1974;8(5):199–211. [PubMed: 4609985]
7. Wisniewski N, Reichert M. *Colloids Surf* 2000;18(3-4):197–219.
8. Dungal P, Long N, Yu B, Moussy Y, Moussy F. *J Biomed Mater Res Part A* 2008;85A:699–706.
9. Koschwanez HE, Reichert WM. *Biomaterials* 2007;28(25):3687–3703. [PubMed: 17524479]
10. Koschwanez HE, Yap FY, Klitzman B, Reichert WM. *J Biomed Mater Res Part A* 2008;87A(3): 792–807.
11. Norton L, Koschwanez H, Wisniewski N, Klitzman B, Reichert W. *J Biomed Mater Res Part A* 2007;81A(4):858–869.

12. Ward WK, Wood MD, Casey HM, Quinn MJ, Federiuk IF. *Diabetes Technol Ther* 2004;6:137–45. [PubMed: 15117580]
13. Hetrick EM, Schoenfisch MH. *Biomaterials* 2007;28(11):1948–1956. [PubMed: 17240444]
14. Mowery KA, Schoenfisch H, M. Saavedra JE, Keefer LK, Meyerhoff ME. *Biomaterials* 2000;21(1):9–21. [PubMed: 10619674]
15. Schoenfisch MH, Mowery KA, Rader MV, Baliga N, Wahr JA, Meyerhoff ME. *Anal Chem* 2000;72(6):1119–1126. [PubMed: 10740848]
16. Schwentker A, Vodovotz Y, Weller R, Billiar TR. *Nitric Oxide* 2002;7(1):1–10. [PubMed: 12175813]
17. Bogdan C. *Nat Immunol* 2001;2:907–16. [PubMed: 11577346]
18. Hetrick EM, Prichard HL, Klitzman B, Schoenfisch MH. *Biomaterials* 2007;28(31):4571–4580. [PubMed: 17681598]
19. Nablo BJ, Prichard HL, Butler RD, Klitzman B, Schoenfisch MH. *Biomaterials* 2005;26(34):6984–6990. [PubMed: 15978663]
20. Amadeu TP, Seabra AB, de Oliveria MG, Costa AM. *J Eur Acad Derm Vener* 2007;21:629–37.
21. Gifford R, Batchelor MM, Lee Y, Gokulrangan G, Meyerhoff ME, Wilson GS. *J Biomed Mater Res Part A* 2005;75A(4):755–766.
22. Bungay PM, Morrison PF, Dedrick RL. *Life Sci* 1990;46:105–19. [PubMed: 2299972]
23. Bungay PM, Newton-Vinson P, Isele W, Garris PA, Justice JB. *J Neurochem* 2003;(86):932–46. [PubMed: 12887691]
24. Stenken JA. *Anal Chim Acta* 1999;379:337–57.
25. Wang X, Lennartz MR, Loegering DJ, Stenken JA. *Anal Chem* 2007;79(5):1816–1824. [PubMed: 17263512]
26. Wisniewski N, Klitzman B, Miller B, Reichert WM. *J Biomed Mater Res* 2001;57(4):513–521. [PubMed: 11553881]
27. Lowry JP, O'Neill RD, Boutelle MG, Fillenz M. *J Neurochem* 1998;70(1):391–396. [PubMed: 9422386]
28. Mou X, Lennartz MR, Loegering DJ, Stenken JA. *Biomaterials* 2010;31(16):4530–4539. [PubMed: 20223515]
29. Stenken JA, Reichert WM, Klitzman B. *Anal Chem* 2002;74(18):4849–4854. [PubMed: 12349994]
30. Bancroft, J.; Gamble, M. *Theory and Practice of Histological Techniques*. 6 ed.. Churchill Livingstone; London: 2007.
31. Badie N, Satterwhite L, Bursac N. *Ann Biomed Eng* 2009;37(12):2510–2521. [PubMed: 19806455]
32. Fischer U, Ertle R, Abel P, Rebrin K, Brunstein E, Dorsche HH, Freyse EJ. *Diabetologia* 1987;30(12):940–945. [PubMed: 3436490]
33. Sharkawy AA, Klitzman B, Truskey GA, Reichert WM. *J Biomed Mater Res* 1997;37(3):401–412. [PubMed: 9368145]
34. Jablecki M, Gough DA. *Anal Chem* 2000;72(8):1853–1859. [PubMed: 10784153]
35. Wilson GS, Hu Y. *Chem Rev* 2000;100(7):2693–2704. [PubMed: 11749301]
36. Schäffer MR, Tantry U, Gross SS, Wasserkrug HL, Barbul A. *Surg Res* 1996;63(1):237–240.
37. Thornton FJ, Schäffer MR, Witte MB, Moldawer LL, MacKay SLD, Abouhamze A, Tannahill CL, Barbul A. *Biochem Biophys Res Commun* 1998;246(3):654–659. [PubMed: 9618268]
38. Schäffer M, Efron P, Thornton F, Klingel K, Gross S, Barbul A. *J Immunol* 1997;158(5):2375–2381. [PubMed: 9036987]
39. Lloyd-Jones MD, Donald M, Bloch MD, Kenneth D. *Annual Review of Medicine* 1996;47(1):365–375.
40. Kurosawa M, Hallström Å, Ungerstedt U. *Neurosci Lett* 1991;126(2):123–126. [PubMed: 1922922]
41. Rosdahl H, Lind L, Millgård J, Lithell H, Ungerstedt U, Henriksson J. *Diabetes* 1998;47(8):1296–301. [PubMed: 9703331]

42. Stenken JA, Lunte CE, Southard MZ, Ståhle L. J Pharm Sci 1997;86(8):958–66. [PubMed: 9269875]

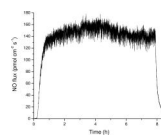


Figure 1.
Representative daily NO release from a microdialysis probe over 8 h while flowing PBS-NO at 2.0 $\mu\text{L}/\text{min}$.

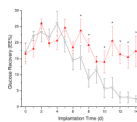


Figure 2. Glucose recovery at various times of implantation for the NO-releasing (filled, red) and control (empty, black) probes. Error bars are \pm standard error of the mean. Significant differences (*) are $p < 0.05$.

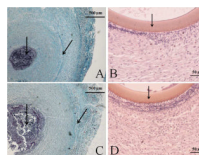


Figure 3. Representative histology slides of cross sections stained with Masson's trichrome (A and C) or hematoxylin and eosin (B and D) of NO-releasing (A and B) and control (C and D) probes explanted at 14 d. Arrows in the hematoxylin and eosin stained pictures indicate the probe membrane. Arrows in the Masson's trichrome stained pictures indicate the implant site, surrounded by dark stained inflammatory cells and the collagen capsule. An increased capsule size and inflammatory response at the membrane surface are observed at control probes.

Table 1

Results of histological analysis from both hematoxylin and eosin and Masson's trichrome stained slides.

Probe type	Cell density (nuclei / 50 × 100 μm ²)	Capsule thickness (μm)	Collagen density (%)
Control (n=5)	60.4 ± 8.9*	689 ± 61 [†]	62 ± 6*
NO-releasing (n=4)	37.7 ± 6.6	599 ± 69	72 ± 4

* Significantly different at p<0.05

[†] Significantly different at p<0.10